

Technical note

Prediction and control of microstructure evolution for sub-microscale α -Al₂O₃ during low-heating-rate sintering based on the master sintering curve theory

W.Q. Shao^a, S.O. Chen^{a,b,*}, D. Li^a, H.S. Cao^a, Y.C. Zhang^a, S.S. Zhang^a

^a College of Physics Science, Qingdao University, Qingdao 266071, PR China

^b Laboratory of Fiber Materials and Modern Textile, the Growing Base for State Key Laboratory, Qingdao University, Qingdao 266071, PR China

Received 10 March 2008; received in revised form 11 June 2008; accepted 11 June 2008

Available online 16 July 2008

Abstract

The master sintering curve (MSC) can sometimes be used for analyzing the shrinkage behaviour of ceramics. Densification of α -Al₂O₃ with the mean particle size of 350 nm was continuously recorded during heating at 0.5, 2 and 5 °C/min. A MSC was successfully constructed using dilatometry data with the help of combined-stage sintering model. The validity of the MSC has been verified by a few experimental runs. The microstructural evolution with densification during different heating-rate sintering was explored. The sintered microstructure is a function of the time–temperature sintering conditions, and it is verified that there exists a link between sintered density and microstructure. The MSC can be used to predict and control microstructure evolution during sintering of α -Al₂O₃ ceramics.

© 2008 Elsevier Ltd. All rights reserved.

Keywords: Sintering; Microstructure-final; Al₂O₃

1. Introduction

In advanced ceramic component manufacturing, reproducible processing of powders was critical for the cost-effective manufacture of reliable ceramic components. Historically, empirical engineering has been used to develop the processes.¹ However, empirical engineering alone cannot provide the fundamental understanding necessary to design new products. Consequently, a different approach is needed to realize the benefits of advanced ceramics. One promising and practical approach to predict and control sintering is based on the concept of the master sintering curve (MSC).² The MSC curve can be used as an aid to compare the sinterability of different powders^{3–5} and to evaluate the apparent activation energy for ceramic sintering.⁶ It also can be used to predict the microstructure evolution because its formulation and construction has been derived from the combined-stage sintering model.⁷ In the MSC

theory, $\Phi(\rho)$ which is function only of density, is given as the function of temperature and time:

$$\Phi(\rho) = \Theta(t, T(t)) = \int_0^t \frac{1}{T} \exp\left(-\frac{Q}{RT}\right) dt \quad (1)$$

where Q is the apparent activation energy for sintering, R the gas constant, T the absolute temperature, t the time. For the master sintering curve, the measured density is plotted as a function of the right-hand side, denoted by Θ . Estimates of Q are biased upwards by the effect of coarsening caused by surface diffusion, particularly at low-heating rates. The MSC for low-heating rates in the presence of low-activation-energy surface diffusion would be biased to higher temperatures from those at higher heating rates. It was found that⁸ the MSCs obtained by sintering at a heating rate of 3–5 °C/min did not correspond to that based on the heating rate of 7.5–20 °C/min.

The objectives of this study were to construct the MSC for α -Al₂O₃ based on non-isothermal sintering containing lower heating rates only. In addition, another objective of the present research are to predict and control microstructure evolution during low-heating-rate sintering of α -Al₂O₃ ceramics.

* Corresponding author at: College of Physics Science, Qingdao University, Qingdao 266071, PR China. Tel.: +86 532 85952321; fax: +86 532 85955977.
E-mail address: shaouchen@126.com (S.O. Chen).

The results demonstrate how MSC theory can be applied to design a reproducible process to fabricate controlled density and microstructure ceramics.

2. Experimental procedure

For constant-heating rate sintering, α - Al_2O_3 powder (99.9% purity, Dalian Luming Nanometer Material Ltd., Dalian, China) with an average particle size of 350 nm was mixed with 1 wt% of adhesion agent, dried, granulated, and screened to -60 mesh. The powder was pressed using a uniaxial pressure of 80 MPa and then further consolidated by cold isostatic pressing at 250 MPa to create bars of $\sim 5 \text{ mm} \times 5 \text{ mm} \times 45 \text{ mm}$. The green density was measured by geometric method. The green density of α - Al_2O_3 powder compacts were $2.08 \pm 0.03 \text{ g/cm}^3$. The value of 3.98 g/cm^3 was used as the theoretical density, which is the monocrystal density.

The shrinkage of α - Al_2O_3 samples were measured with a push rod type dilatometer in axial direction (Luoyang Anter-Lirr Instrument Co., Ltd., RPZ-03P, Luoyang, China). The length change measurements were made by a linear voltage differential transducer (LVDT) which was maintained at a constant temperature by means of water circulation from a constant temperature bath. The accuracy of the measurement of change in length was within $\pm 0.1 \mu\text{m}$. The temperature was measured using a calibrated thermocouple which is placed directly above the sample.

Firstly, three green compacts were heated to the peak temperature of 1640°C at the heating rates of 0.5, 2 and 5°C/min . Secondly, other runs for non-isothermal sintering were carried out in the same system by heating at 1°C/min to 1115°C , 2°C/min to 1250°C , 3°C/min to 1420°C , 4°C/min to 1575°C and 5°C/min to 1650°C without holding dwell time, respectively. To ensure experimental consistency, typically, three samples were characterized at each heating rate. Apparent densities of the sintered samples were determined by the Archimedes method. The microstructures of the specimens were examined by scanning electron microscopy (JSM-6390LV, JEOL, JAPAN). The average grain size of sintered samples was determined by the software for image analysis (Nanjing East-image Digital Technology Co., Ltd., DT2000, Nanjing, China). The principle of grain size measurement by the image analysis software is the mean linear intercept method. The average grain size was calculated by multiplying the mean linear intercept by 1.5. More than 300 intercepts were measured for each sample.

3. Results and discussion

3.1. MSC construction

For the construction of MSC, the integral of Eq. (1) and the experimental density should be known. Fig. 1 shows the time-dependent relative density (converted from the dilatometer data using a certain relation⁹) versus temperature. For the calculation of Θ , the activation energy must be known. If the activation energy is unknown, it can be estimated with good precision from Θ versus density (ρ) data.² The apparent activation energy for

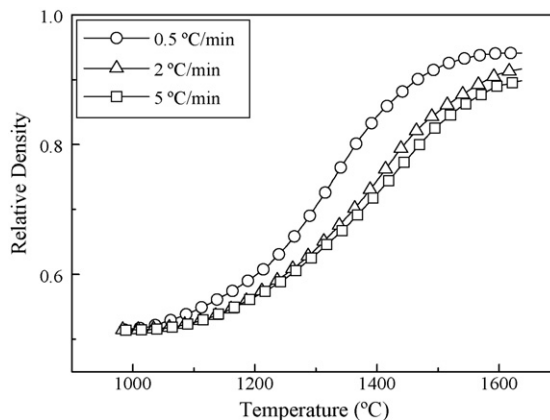


Fig. 1. Relative density as a function of sintering temperature.

the MSC of densification are determined by minimising mean residual method. The mean residual used is defined as follows¹⁰:

mean residual

$$= \sqrt{\frac{1}{\rho_f - \rho_i} \int_{\rho_i}^{\rho_f} \frac{\sum_{m=1}^N ((\Theta_m - \Theta_{\text{avg}}) - 1)^2}{N} d\rho} \quad (2)$$

where m is the dummy variable for summation, N is the number of experimental data, Θ_{avg} is the average value of work of sinterings at density for m th experiment, Θ_m is the work of sintering for m th experiment, and ρ_i is the initial density, and ρ_f is the final density, respectively.

For this purpose, initially, an estimate is made for the activation energy Q , and the MSCs for three heating profiles are computed using Eq. (1). If the correct value of Q has been given, all of the data converge to a single curve. A curve (a polynomial function) can be fitted to all the data points, and then the convergence of the data to the fitted line can be quantified through the sum of the residual squares of the points with respect to the fitted line. Another estimate of Q is made, and the process is repeated. When the best estimate of Q is found, the mean residual is a minimum. The minimum is reached at $\sim 1064 \text{ kJ/mol}$, indicating the estimated sintering activation energy. From the knowledge of the activation energy of sintering obtained above, MSC for α - Al_2O_3 has been constructed and is shown in Fig. 2.

It should be noted that the activation energy value obtained in the present work is quite high, which is twice as high as 555 kJ/mol obtained by Tatami et al. (samples were heated to 1400°C at constant heating rates of 5, 10 and 20°C/min)⁸ or Wang and Raj¹¹ of 440 kJ/mol (samples were raised to 800°C in 1 h and held at that temperature for 10 min, and then heated to 1600°C using the heating rates of 5, 10 and 20°C/min). However, the activation energy of 1064 kJ/mol obtained in the present work is similar to 1080 kJ/mol in the literature (three heating rates of 3, 5, and 10°C/min were used to reach the desired temperature of 1700°C without holding).¹² The value obtained for Q can vary drastically, depending on the conditions (i.e., the characteristics of the raw materials, the preparing procedure of green compacts, the sintering procedure, etc.) under which the sintering data are obtained.

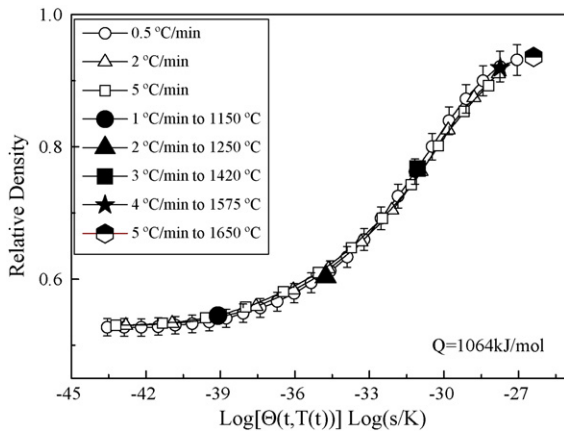


Fig. 2. Validation of master sintering curve for α -Al₂O₃ (including error bars). The density determined by dilatometer trace agreed well with Archimedes density.

3.2. MSC validation

Fig. 2 shows the relative density continuously determined by dilatometer during sintering with constant heating rate as well as those measured by Archimedes method after sintering with different heating profiles. The relative densities from dilatometer trace (53.3, 61, 75.9, 90.8, 92.9%) are consistent well with those determined by Archimedes method (54.5, 60.4, 76.7, 91.9, 93.6%) after different sintering process (1 °C/min to 1115 °C, 2 °C/min to 1250 °C, 3 °C/min to 1420 °C, 4 °C/min to 1575 °C and 5 °C/min to 1650 °C). The relatively small error bars (2.5%) on the MSC for 350 nm α -alumina shown in Fig. 2 are indicative of the small and apparently random scatter of the sintering data about the MSC. The small error could be attributed to the fact that the calculated density values from the dilatometer results were calculated at a specific temperature, while the Archimedes measurements were made at room temperature.

3.3. Microstructure evolution prediction using MSC

Fig. 3(a)–(e) shows SEM micrographs of the fractured surfaces of the specimens undergoing different heating history. Based on SEM images, the microstructure is characterized by the presence of finer α -Al₂O₃ particles (200 nm) in Fig. 3(a) and (b) and coarser particles (400 nm) in Fig. 3(c). The Archimedes densities of samples by heating at 1 °C/min to 1115 °C, 2 °C/min to 1250 °C and 3 °C/min to 1420 °C without holding dwell time were determined to be 2.17 ± 0.02 , 2.4 ± 0.01 and 3.05 ± 0.04 g/cm³, respectively. A comparison of Fig. 3(d) and (e) indicates that the density for specimen by heating at 4 °C/min to 1575 °C are relatively lower (3.66 ± 0.05 g/cm³) than that for the specimen by heating at 5 °C/min to 1650 °C (3.73 ± 0.03 g/cm³). The average grain size in Fig. 3(d) are determined to be 2 μ m, while the presence of coarser grains of sizes 3 μ m or more can be noted in Fig. 3(e). Moreover, the fractographs reveal the transgranular fracture of specimens in Fig. 3(d) and (e), and predominantly intergranular fracture of samples in Fig. 3(a)–(c).

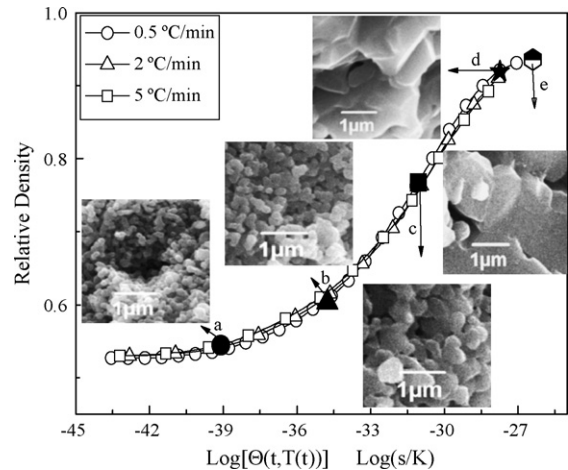


Fig. 3. The microstructure evolution of samples sintered in different sintering profiles in MSC curve. (a) 1 °C/min to 1115 °C, (b) 2 °C/min to 1250 °C, (c) 3 °C/min to 1420 °C, (d) 4 °C/min to 1575 °C and (e) 5 °C/min to 1650 °C.

Fig. 3 shows the microstructure evolution in different sintering profiles in MSC curve. If the heating profiles are given, the Θ value can be calculated by Eq. (1). Then, according to Fig. 3, it is possible to predict the final relative density and microstructure of samples sintered in different heating profiles. On the other hand, the Θ value can be determined according to the required density and microstructure. Then, the heating procedure can be determined.

4. Conclusions

The densification of α -alumina with 350 nm of average grain size in diameter was studied by low-heating-rate pressureless sintering. The density continuously determined by dilatometer during sintering was plotted against the integral of a temperature function over time, $\Theta(t, T(t))$. It agreed well with the densities determined by Archimedes method after sintering with different heating history. Moreover, the MSC can also be used to predict and control microstructure evolution during sintering of α -Al₂O₃ ceramics. Therefore, MSC theory can be applied to design a reproducible process to fabricate α -Al₂O₃ ceramics with controlled density and microstructure.

Acknowledgment

This work was supported by Qingdao Nature Science Foundation No. 05-1-JC-89, P R China.

References

- Ewsuk, K. G., Argüello, J. G., Zeuch, D. H., Farber, B., Carinci, L., Kaniuk, J. et al., CRADA develops model for powder pressing and die design. Part 1. *Bull. Am. Ceram. Soc.*, 2001, **80**, 53–60.
- Su, H. and Johnson, D. L., Master sintering curve: a practical approach to sintering. *J. Am. Ceram. Soc.*, 1996, **79**, 3211–3217.
- Ewsuk, K. G., Ellerby, D. T. and DiAntonio, C. B., Analysis of nanocrystalline and microcrystalline ZnO sintering using master sintering curves. *J. Am. Ceram. Soc.*, 2006, **89**, 2003–2009.

4. Nikolic, M. V., Pavlovic, V. P., Labus, N. and Stojanovic, B., Application of the master sintering curve theory to non-isothermal sintering of BaTiO₃ ceramics. *Mater. Sci. Forum*, 2005, **494**, 417–422.
5. Diantonio, C. B. and Ewsuk, K. G., Controlled and predicted ceramic sintering through master sintering curve theory. *Ceram. Trans.*, 2005, **157**, 15–23.
6. Kutty, T. R. G., Khan, K. B., Hegde, P. V., Banerjee, J., Sengupta, A. K., Majumdar, S. et al., Development of a master sintering curve for ThO₂. *J. Nucl. Mater.*, 2004, **327**, 211–219.
7. Hansen, J., Rusin, R. P., Teng, M. and Johnson, D. L., Combined-stage sintering model. *J. Am. Ceram. Soc.*, 1992, **75**, 1129–1135.
8. Tatami, J., Suzuki, Y., Wakihara, T., Meguro, T. and Komeya, K., Control of shrinkage during sintering of alumina ceramics based on master sintering curve theory. *Key Eng. Mater.*, 2006, **317–318**, 11–14.
9. Xiong, X. D., Sintering behavior of pure hafnium oxide. *Rare Met. Mater. Eng.*, 1999, **28**, 298–301.
10. Park, S. J. and German, R. M., Master curves based on time integration of thermal work in particulate materials. *Int. J. Mater. Struct. Integrity*, 2007, **1**, 128–147.
11. Wang, J. D. and Raj, R., Estimate of the activation energies for boundary diffusion from rate-controlled sintering of pure alumina, and alumina doped with zirconia or titania. *J. Am. Ceram. Soc.*, 1990, **73**, 1172–1175.
12. Fang, T. T., Shive, J. T. and Shiau, F. S., On the evaluation of the activation energy of sintering. *J. Mater. Chem. Phys.*, 2003, **80**, 108–113.